Radiation Protection Dosimetry (2004), Vol. 110, Nos 1-4, pp. 249–254
doi:10.1093/rpd/nch222

ANDI-03: A GENETIC ALGORITHM TOOL FOR THE ANALYSIS OF ACTIVATION DETECTOR DATA TO UNFOLD HIGH-ENERGY NEUTRON SPECTRA

Bhaskar Mukherjee
Deutsches Elektronen-Synchrotron (DESY), Notkestrasse 85, D-22607 Hamburg, Germany

The thresholds of (n,xn) reactions in various activation detectors are commonly used to unfold the neutron spectra covering a broad energy span, i.e. from thermal to several hundreds of MeV. The saturation activities of the daughter nuclides (i.e. reaction products) serve as the input data of specific spectra unfolding codes, such as SAND-II and LOUHI-83. However, most spectra unfolding codes, including the above, require an *a priori* (guess) spectrum to starting up the unfolding procedure of an unknown spectrum. The accuracy and exactness of the resulting spectrum primarily depends on the subjectively chosen guess spectrum. On the other hand, the Genetic Algorithm (GA)-based spectra unfolding technique ANDI-03 (Activation-detector Neutron DIfferentiation) presented in this report does not require a specific starting parameter. The GA is a robust problem-solving tool, which emulates the Darwinian Theory of Evolution prevailing in the realm of biological world and is ideally suited to optimise complex objective functions globally in a large multidimensional solution space. The activation data of the ^{27}Al(n,α)^{24}Na, ^{116}In(n,γ)^{116m}In, ^{12}C(n,2n)^{11}C and ^{209}Bi(n,xn)$^{210-x}$Bi reactions recorded at the high-energy neutron field of the ISIS Spallation source (Rutherford Appleton Laboratory, UK) was obtained from literature and by applying the ANDI-03 GA tool, these data were used to unfold the neutron spectra. The total neutron fluence derived from the neutron spectrum unfolded using GA technique (ANDI-03) agreed within $\pm$6.9% (at shield top level) and $\pm$27.2% (behind a 60 cm thick concrete shield) with the same unfolded with the SAND-II code.

INTRODUCTION

The neutron spectrum unfolding using Bonner spheres and/or Activation foils requires the solution of Fredholm's integral equation (FIE) of the first kind. The FIE has no unique solution and an *a priori* (guess) solution is required to initiate the computation. The spectra unfolding technique belongs to category of inverse problem, i.e. a spectrum of interest, with a large number of bins is estimated (unfolded) using the input data collected from a few number of detectors[1]. Equation 1 represents a multibin neutron spectrum in matrix form as described by the FIE.

$$(c_1 c_2 \ldots c_n \ldots c_j) = \begin{pmatrix} r_{11} & r_{12} & \ldots & r_{1n} & \ldots & r_{1j} \\ r_{21} & r_{22} & \ldots & r_{2n} & \ldots & r_{2j} \\ \vdots & \vdots & & \vdots & & \vdots \\ r_{m1} & r_{m2} & \ldots & r_{mn} & \ldots & r_{mj} \\ \vdots & \vdots & & \vdots & & \vdots \\ r_{i1} & r_{i2} & \ldots & r_{in} & \ldots & r_{ij} \end{pmatrix} \bullet \begin{pmatrix} \phi_1 \\ \phi_2 \\ \vdots \\ \phi_m \\ \vdots \\ \phi_i \end{pmatrix}, \quad (1)$$

where, the left-hand side, the 1st part of the right-hand side and the 2nd part of the right-hand side of Equation 1 represent the detector counts, the response matrix of the detectors and the fluence vector (neutron spectrum), respectively. The indices for the neutron energy bins and detector types are represented by '*i*' and '*j*' respectively.

NEUTRON SPECTRA UNFOLDING USING A GENETIC ALGORITHM

A Genetic Algorithm (GA) is a mathematical technique, which emulates the paradigm of biological evolution[2,3] prevails in the realm of nature. The theory of evolution was postulated by 19th century British naturalist Sir Charles Darwin[4]. A GA is ideally suited to search for the best (globally optimised) solution from a large multidimensional solution space[3]. The principle of a GA-based optimisation technique is highlighted below:
Step 1: Generation of a large number of prospective solutions as binary strings at random. *Step 2*: Estimation of the deviation of each solution (fitness test) from a pre-selected parameter (Goal). *Step 3*: Selection of the best (fittest) solutions, i.e. closest to the pre-set parameter and rejection of the rest. *Step 4*: Selection of pairs of best solution (parent chromosome) at random and exchange (crossover) of a selected group of bits (Gene) among the pair to produce new solution pair (offspring). *Step 5*: Continuation of the Loop. *Steps 2–5* until a population of ~100% best (fittest) solutions is achieved[5].

Corresponding author: mukherjee@ieee.org

The solution of the FIE (i.e. unfolding of a neutron spectrum) using the GA technique summarised as follows: by manipulating each component using a GA the neutron fluence vector $\langle \phi_i \rangle$ in Equation 1 is globally optimised and the corresponding detector output (i.e. pulse count) of each detector (c_j) is explicitly (inverse) calculated until the criteria 2a and 2b are met.

$$\left|\left(c_{\mathrm{meas}(n)}/c_{\mathrm{calc}(n)}\right)\right|_{n=1}^{n=j} \sim 1 \tag{2a}$$

$$|\phi_m|_{m=1}^{m=i} > 0 \tag{2b}$$

The implications of the above expressions are: (a) the calculated pulse count of each detector shall be equal to the measured pulse count and (b) the fluence vector shall have only positive, no-zero elements. The fluence vector $\langle \phi_i \rangle$ represents the unfolded neutron spectrum (i.e. the optimal solution of the FIE) when the above conditions are satisfied[6].

MATERIALS AND METHODS

The data obtained from an extensive shielding experiment carried out at the high-energy spallation neutron source of the Rutherford Appleton Laboratory (RAL) was used to unfold the neutron spectrum. An 800 MeV H^+ beam at 170 μA from the ISIS proton synchrotron bombarded a thick tantalum target to produce intense beam of fast neutrons via the spallation process. Neutrons emerging at 90° with the primary proton beam reach the shield top level above the tantalum target after

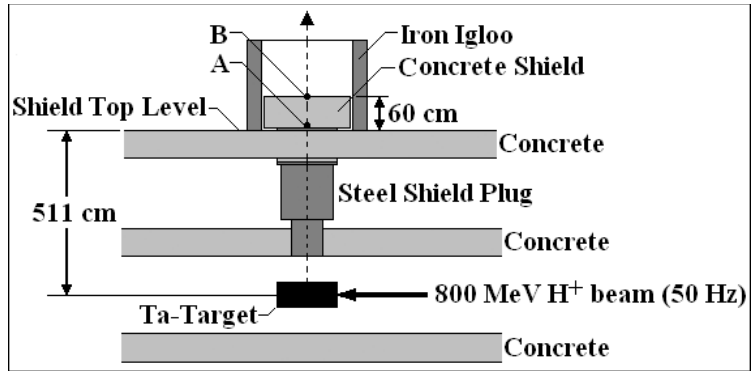

Figure 1. Shown is the shielding arrangement of the spallation neutron production target at the ISIS proton synchrotron of RAL, UK. The diagram has been explained in the text.

Table 1. Showing the activation detectors with the characteristic nuclear reactions and the corresponding reaction rate (detector output) recorded at the shield top level (Position A) and after 60 cm thick concrete shield (Position B) (Figure 1).

Activation detector (nuclear reaction)	Reaction rate [atom^{-1} Coulomb^{-1}]	
	Shield top level	Behind 60 cm concrete
$^{27}Al(n,\alpha)^{24}Na$	1.25E−20 ± 4.48%	3.09E−21 ± 4.90%
$^{12}C(n,2n)^{11}C$	6.75E−21 ± 2.57%	2.04E−21 ± 4.57%
$^{116}In(n,\gamma)^{116}In^m$ (19.6 cm diam.)	3.77E−16 ± 2.37%	4.58E−17 ± 5.81%
$^{116}In(n,\gamma)^{116}In^m$ (11.0 cm diam.)	5.34E−16 ± 2.17%	9.22E−17 ± 4.08%
$^{116}In(n,\gamma)^{116}In^m$ (6.4 cm diam.)	2.65E−16 ± 2.39%	6.29E−17 ± 6.14%
$^{116}In(n,\gamma)^{116}In^m$ (4.1 cm diam.)	9.04E−17 ± 4.18%	3.88E−17 ± 6.14%
$^{116}In(n,\gamma)^{116}In^m$ (0 cm diam.)	2.35E−17 ± 7.80%	1.94E−17 ± 8.29%
$^{209}Bi(n,4n)^{206}Bi$	1.00E−19 ± 11.9%	2.86E−20 ± 22.6%
$^{209}Bi(n,5n)^{205}Bi$	9.18E−20 ± 20.8%	2.60E−20 ± 25.1%
$^{209}Bi(n,6n)^{204}Bi$	5.31E−20 ± 5.10%	1.63E−20 ± 8.3%
$^{209}Bi(n,7n)^{203}Bi$	4.40E−20 ± 16.4%	1.40E−20 ± 32.6%
$^{209}Bi(n,8n)^{202}Bi$	2.74E−20 ± 10.1%	9.33E−21 ± 17.0%
$^{209}Bi(n,9n)^{201}Bi$	1.69E−20 ± 24.8%	5.75E−21 ± 40.8%
$^{209}Bi(n,10n)^{200}Bi$	8.48E−21 ± 23.9%	3.56E−21 ± 28.1%

The data was adopted from the literature[7].

penetrating through a combination of concrete and steel shielding. The neutron spectrum at various shielding modalities was evaluated using different types activation detectors. The detectors were placed at the shield top level housed in an iron igloo. The full details of the shielding experiment and the results were reported elsewhere[7]. In this work, the neutron spectrum at shield top level (position A) and after a 60 cm thick concrete shield (position B) was evaluated (Figure 1) using a GA. The activation detectors and the indium-loaded multimoderator detectors used in this unfolding code and the corresponding reaction rates are shown in Table 1.

A GA-based neutron spectrum unfolding tool ANDI-03 (Activation-detector Neutron DIfferentiation using a GA) has been developed with a minor modification of the Bonner sphere version of the spectra unfolding code reported elsewhere[5,6]. The GA code ANDI-03 was written in Microsoft Excel V7.0 environment (as a macro program) to drive the commercially available GA search Engine[5] EVOLVER Version 4.0. An initial organism population (i.e. prospective solutions generated at random) of 100 with the crossover and mutation rates of 0.5 and 0.06, respectively, were used. The initial guess spectrum was set as a step function of amplitude of 100. Furthermore, each spectrum was unfolded 11 times by varying the measured detector counts in 10 steps within the span of experimental error ($\pm\sigma$) as shown in Equation 3.

$$c_{\mathrm{nk}} = c_{\mathrm{meas}}(n) + k\sigma, \tag{3}$$

where c_{nk}, $c_{\mathrm{meas}(n)}$ and k represent the counts of nth-detector used in unfolding procedure, measured counts of the nth-detector and the step-factor, respectively. The running values of k were set as: -1.0, -0.8, -0.6, -0.4, -0.2, 0.0, $+0.2$, $+0.4$, $+0.6$, $+0.8$ and $+1.0$.

RESULTS AND DISCUSSION

In Figure 2, the neutron spectra at two different locations, unfolded using the ANDI-03 GA tool are shown with the same spectra unfolded with the SAND-II code[7]. The reliability of the ANDI-03 GA tool was evidently verified by the 'inverse calculation' of each detector output from the unfolded neutron spectra. The average values of the measured and 'inverse calculated' detector count ratio

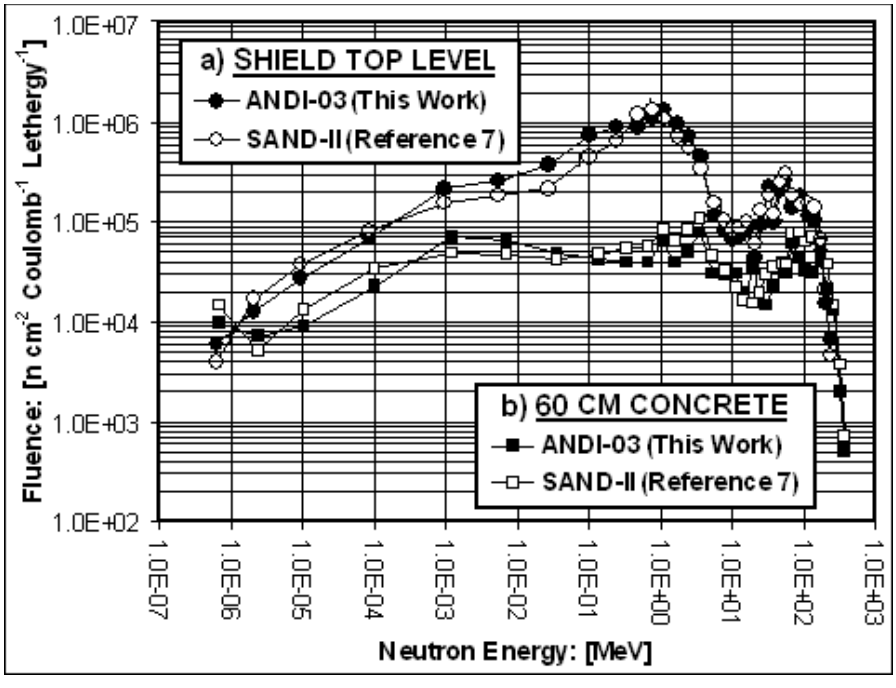

Figure 2. Neutron energy spectrum of the spallation-neutron production target (Figure 1) unfolded with ANDI-03 GA and SAND-II codes at (a) shield top level, ANDI-03 (full circles), SAND-II (hollow circles) and (b) behind 60 cm concrete shield, ANDI-03 (full squares) and SAND-II (hollow squares). Each data point (ANDI-03) represents the average of neutron fluence derived from 11 unfolded spectra.

($C_{Measured}/C_{Calculated}$), derived from 11 unfolded spectra are shown in Table 2. The average count ratio $(C_{Measured}/C_{Calculated})_{AV}$ was plotted with the corresponding detector type and found to be close to unity, $1.0 \pm 10\%$ (Figure 3). This validates the main goal of the GA-based spectra unfolding technique as described in Expression 2a. The neutron energy distribution unfolded with a GA (ANDI-03) and SAND-II[7] code at shield top plate and behind the 60 cm thick concrete shield are shown in Table 3.

Table 2. The average ratio $(C_{Measured}/C_{Calculated})_{AV}$ of the measured and calculated detector counts at position A (shield top level) and position B (behind 60 cm thick concrete shield) and the corresponding standard deviation ($\pm\sigma$ %) are shown with the corresponding detector type.

Activation detector (nuclear reaction)	$(C_{Measured}/C_{Calculated})_{AV}$			
	Position A	σ [±%]	Position B	σ [±%]
$^{27}Al(n,\alpha)^{24}Na$	1.01E+00	2.7	1.01E+00	1.8
$^{12}C(n,2n)^{11}C$	9.54E−01	1.6	9.44E−01	3.7
$^{116}In(n,\gamma)^{116}In^{m}$ (19.6 cm diam.)	1.00E+00	3.2	9.40E−01	1.7
$^{116}In(n,\gamma)^{116}In^{m}$ (11.0 cm diam.)	1.01E+00	1.4	1.08E+00	1.3
$^{116}In(n,\gamma)^{116}In^{m}$ (6.4 cm diam.)	1.02E+00	2.1	9.64E−01	3.4
$^{116}In(n,\gamma)^{116}In^{m}$ (4.1 cm diam.)	9.85E−01	2.2	1.01E+00	2.2
$^{116}In(n,\gamma)^{116}In^{m}$ (0 cm dia)	1.02E+00	3.2	9.81E−01	2.3
$^{209}Bi(n,4n)^{206}Bi$	1.03E+00	1.7	1.02E+00	5.8
$^{209}Bi(n,5n)^{205}Bi$	1.01E+00	3.5	1.02E+00	4.9
$^{209}Bi(n,6n)^{204}Bi$	1.05E+00	2.0	1.05E+00	3.3
$^{209}Bi(n,7n)^{203}Bi$	9.43E−01	2.7	9.40E−01	14.4
$^{209}Bi(n,8n)^{202}Bi$	1.06E+00	6.5	1.06E+00	7.6
$^{209}Bi(n,9n)^{201}Bi$	1.00E+00	4.0	9.62E−01	19.2
$^{209}Bi(n,10n)^{200}Bi$	1.01E+00	4.0	1.01E+00	9.3

The main sources of uncertainty in the unfolded neutron spectrum and the ($C_{Measured}/C_{Calculated}$) ratio (Table 2) were the inaccuracy of the detector response matrix (Equation 1) and experimental error of the measured detector counts (Table 1). The scatter of the average ratio $(C_{Measured}/C_{Calculated})_{AV}$ confirmed the above facts (Figure 3 and Table 2).

There was neither a smoothing of the data points at high-energy region (cascade) of unfolded spectra (Figure 2) nor an paper propagation analysis available for the reference spectra[7]. Hence, in this paper, the difference in the neutron fluence for every single neutron energy bin estimated by SAND-II and ANDI-03 unfolding methods are presented (Table 3). Although there was a strong fluctuation in neutron fluence (columns 4 and 7 of Table 3), the total neutron fluence (Φ_{Total}) derived from both methods matched well with each other. The differences constitute 6.9% (column 4 of the last row in Table 3) and 27.2% (column 7 of the last row in Table 3) for the unfolded neutron spectra at shield top level and behind the 60 cm concrete shield, respectively. It has been planned to include a comprehensive error propagation analysis[1] in the ANDI-03 spectra unfolding routine in the near future.

The GA is a global optimisation process[3]; hence, the introduction of a special *a priori* spectrum (i.e. Maxwellian) to start up the spectra unfolding

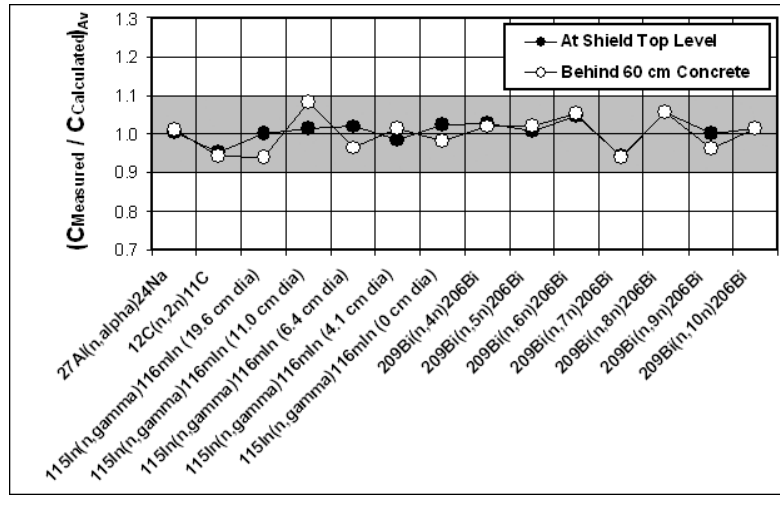

Figure 3. The average ratio $(C_{Measured}/C_{Calculated})_{AV}$ of the measured and calculated detector counts are plotted against the corresponding activation detector. Each data point represents the average ratio derived from 11 individual unfolded spectra. All data points are found to be within the $1.0 \pm 10\%$ band.

Table 3. Showing the neutron fluence (n cm^{-2} Coulomb^{-1} Lethergy^{-1}) at shielding top level (position A) and behind the 60 cm concrete shield (position B) with the corresponding neutron energy (*E*n) unfolded using ANDI-03 (this work) and SAND II[7] codes.

E_n [MeV]	Neutron fluence (position A)			Neutron fluence (position B)		
	ANDI-03	SAND-II	Difference [±%]	ANDI-03	SAND-II	Difference [±%]
6.81E−07	5.20E+03	3.42E+03	4.13E+01	1.00E+04	1.45E+04	3.67E+01
2.38E−06	1.13E+04	1.55E+04	3.13E+01	7.00E+03	5.12E+03	3.10E+01
1.07E−05	2.51E+04	3.53E+04	3.39E+01	9.00E+03	1.30E+04	3.64E+01
1.01E−04	6.50E+04	7.72E+04	1.72E+01	2.30E+04	3.42E+04	3.92E+01
1.23E−03	2.05E+05	1.47E+05	3.30E+01	7.10E+04	4.81E+04	3.85E+01
7.09E−03	2.50E+05	1.81E+05	3.20E+01	6.50E+04	4.65E+04	3.32E+01
3.60E−02	3.61E+05	2.11E+05	5.24E+01	4.81E+04	4.26E+04	1.21E+01
1.39E−01	7.44E+05	4.36E+05	5.21E+01	4.18E+04	4.76E+04	1.31E+01
3.34E−01	8.80E+05	6.46E+05	3.07E+01	4.00E+04	5.39E+04	2.96E+01
6.72E−01	9.00E+05	1.19E+06	2.78E+01	4.00E+04	5.69E+04	3.49E+01
1.11E+00	1.06E+06	1.36E+06	2.45E+01	6.50E+04	8.40E+04	2.55E+01
1.65E+00	1.35E+06	1.06E+06	2.40E+01	4.00E+04	6.52E+04	4.79E+01
2.47E+00	9.73E+05	7.07E+05	3.17E+01	5.00E+04	8.37E+04	5.04E+01
3.68E+00	7.00E+05	5.30E+05	2.76E+01	8.00E+04	1.09E+05	3.07E+01
5.48E+00	4.30E+05	3.40E+05	2.35E+01	3.00E+04	4.53E+04	4.06E+01
8.19E+00	1.10E+05	1.48E+05	2.95E+01	2.96E+04	3.33E+04	1.17E+01
1.16E+01	7.50E+04	9.95E+04	2.81E+01	3.00E+04	2.17E+04	3.21E+01
1.54E+01	6.20E+04	7.83E+04	2.32E+01	2.00E+04	1.67E+04	1.80E+01
1.98E+01	6.67E+04	8.20E+04	2.06E+01	3.50E+04	1.50E+04	8.00E+01
2.49E+01	7.60E+04	9.57E+04	2.29E+01	1.50E+04	1.95E+04	2.61E+01
3.10E+01	4.10E+04	5.65E+04	3.18E+01	1.48E+04	2.95E+04	6.66E+01
3.97E+01	8.94E+04	1.21E+05	3.00E+01	2.30E+04	3.57E+04	4.33E+01
4.97E+01	2.18E+05	1.78E+05	2.02E+01	4.00E+04	3.76E+04	6.19E+00
5.98E+01	9.10E+04	1.15E+05	2.33E+01	3.00E+04	3.82E+04	2.40E+01
7.21E+01	1.96E+05	2.42E+05	2.10E+01	6.00E+04	7.69E+04	2.47E+01
8.94E+01	2.50E+05	3.01E+05	1.85E+01	4.33E+04	7.89E+04	5.83E+01
1.10E+02	1.31E+05	1.79E+05	3.11E+01	3.33E+04	6.21E+04	6.04E+01
1.39E+02	1.80E+05	1.43E+05	2.29E+01	3.20E+04	6.97E+04	7.41E+01
1.79E+02	1.12E+05	1.49E+05	2.84E+01	4.00E+04	6.10E+04	4.16E+01
2.24E+02	9.80E+04	1.33E+05	3.03E+01	2.10E+04	3.76E+04	5.67E+01
2.74E+02	4.60E+04	6.35E+04	3.20E+01	1.30E+04	1.48E+04	1.29E+01
3.24E+02	1.35E+04	1.88E+04	3.26E+01	2.00E+03	3.75E+03	6.09E+01
3.74E+02	5.88E+03	3.97E+03	3.88E+01	5.00E+02	7.14E+02	3.53E+01
Φ_{Total}	9.82E+06	9.15E+06	6.89E+00	1.10E+06	1.40E+06	2.72E+01

The last row highlights the total neutron fluence (Φ_{Total}) derived from both methods.

process had no influence in the final result, except a minor reduction of computing time. This work demonstrated the successful application of a GA to unfold high-energy neutron spectrum using different types of activation detectors.

ACKNOWLEDGEMENTS

Author wishes to thank Prof. Takashi Nakamura and Dr Tomoya Nunomya of Thohoku University, Sendai, Japan for supplying the data used in this report, and Dr Reginald M. Ronningen of National Superconducting Cyclotron Laboratory (NSCL), Michigan State University, East Lansing, USA for many valuable discussions.

REFERENCES

1. Matzke, M. *Propagation of uncertainties in unfolding procedures*. Nucl. Instrum. Meth. Phys. Res. A **476**, 230–241 (2002).
2. Holland, J. H. *Adaptation in Natural and Artificial Systems* (Ann Arbour: University of Michigan Press) (1975).
3. Goldberg, D. E. *Genetic Algorithms in Search, Optimization and Machine Learning* (Massachusetts: Addison-Wesley, Reading) (1989).

4. Darwin, C. *The Origin of Species* (London: Watts and Co.) (1929).
5. Mukherjee, B. *BONDI-97: a novel neutron energy spectrum unfolding tool using a genetic algorithm*. Nucl. Instrum. Meth. Phys. Res. A **432**, 305–312 (1999).
6. Mukherjee, B. *A high resolution neutron spectra unfolding method using the Genetic Algorithm technique*. Nucl. Instrum. Meth. Phys. Res. A **476**, 247–251 (2002).
7. Nunomiya ,T. and 12 others. *Experimental data of deep-penetration neutrons through a concrete and iron shield at the ISIS spallation neutron source facility using an 800-MeV proton beam.* KEK Report 2001–24, 25 February (2002).